



## Bonding strength of Invar/Cu clad strips fabricated by twin-roll casting process

Peng CHEN<sup>1,2</sup>, Hua-gui HUANG<sup>1,2</sup>, Ce JI<sup>1,2</sup>, Xu ZHANG<sup>1,2</sup>, Zhong-hua SUN<sup>3</sup>

1. National Engineering Research Center for Equipment and Technology of Cold Strip Rolling, Yanshan University, Qinhuangdao 066004, China;
2. College of Mechanical Engineering, Yanshan University, Qinhuangdao 066004, China;
3. Iron and Steel Research Institute of HBIS Group, Shijiazhuang 052165, China

Received 23 October 2017; accepted 6 June 2018

**Abstract:** Based on traditional twin-roll casting process, Invar/Cu clad strips were successfully fabricated by using solid Invar alloy strip and molten Cu under conditions of high temperature, high pressure and plastic deformation. A series of tests including tensile test, bending test, T-type peeling test and scanning electron microscope (SEM) and energy dispersive spectrometer (EDS) measurements were carried out to analyze the mechanical properties of Invar/Cu clad strips and the micro-morphology of tensile fracture surfaces and bonding interfaces. The results indicate that no delamination phenomenon occurs during the compatible deformation of Invar/Cu in bending test and only one stress platform exists in the tensile stress–strain curve when the bonding strength is large. On the contrary, different mechanical properties of Invar and Cu lead to delamination phenomenon during the uniaxial tensile test, which determines that two stress platforms occur on the stress–strain curve of Invar/Cu clad strips when two elements experience necking. The average peeling strength can be increased from 13.85 to 42.31 N/mm after heat treatment at 800 °C for 1 h, and the observation of the Cu side at peeling interface shows that more Fe is adhered on the Cu side after the heat treatment. All above illustrate that heat treatment can improve the strength of the bonding interface of Invar/Cu clad strips.

**Key words:** twin-roll casting; Invar/Cu clad strip; heat treatment; bonding interface; bonding strength

### 1 Introduction

As structural and functional materials, bimetal clad strips are capable of combining the properties of dissimilar metals and making economic benefits via replacing expensive metals with cheap ones [1,2]. They have been widely used in many fields, such as in chemical industry, heat exchangers and electrical technologies, kitchen utensils, automotive and shipbuilding industries as well as manufacturing household appliances [3–5].

Various techniques were proposed to fabricate bimetallic clad strips [6–9], such as diffusion bonding [10], roll bonding [11, 12], explosive welding [13], and friction-stir welding [14]. At present, compared with other methods, roll bonding has been most frequently used due to its low cost and high productivity. However, an inheriting problem of

traditional roll bonding is that the rolling reduction is usually no less than 60%, which highly lowers working efficiency and increases energy consumption. Therefore, the twin-roll casting technology was proposed to save more energy and meet space requirements [15,16]. It has been proved that metal clad strips with sound bonding strength can be achieved via the twin-roll casting process [17,18]. In addition, clad strips with the combination of various materials have been fabricated, such as Cu/Al [19,20], Al/Mg [21], steel/Al [22,23], Ti/Al [24], austenitic stainless steel/carbon steel [25] and high manganese steel/stainless steel [26].

To meet the requirements of the new electronic packaging materials, Invar/Cu strips are in great demand. In order to achieve Invar/Cu strips, Invar/Cu composites with low expansion and high thermal conductivity were firstly synthesized by powder metallurgy [27–29], and then layered Invar/Cu strips could be fabricated via cold rolling. However, some key issues on Invar/Cu

**Foundation item:** Project (51474189) supported by the National Natural Science Foundation of China; Project (E2018203446) supported by the Excellent Youth Foundation of Hebei Scientific Committee, China; Project (QN2015214) supported by the Educational Commission of Hebei Province, China

**Corresponding author:** Hua-gui HUANG; Tel: +86-335-8077352; E-mail: [hhg@ysu.edu.cn](mailto:hhg@ysu.edu.cn)  
DOI: 10.1016/S1003-6326(18)64892-7

composites are presented: (1) In the powder metallurgy process, high sintering temperature is required to obtain the high-density composites, but interdiffusion at interface is increased significantly as the temperature rises, resulting in the physical properties deterioration of materials; (2) For Invar/Cu clad strip obtained via cold rolling, the weak interface bonding strength is the fatal disadvantage, which may loosen or even separate the bonding materials and cause great defects [30,31].

Until now, there has been no report for solving the aforementioned issues of Invar/Cu composites by twin-roll casting process. In this work, Invar/Cu clad strips were fabricated by twin-roll casting process. The compatible deformation of as-cast clad strips was evaluated by tensile test and bending test. And the interface bonding strength of the as-cast strips and those subjected to further heat treatment were investigated by peeling test. After the tests, the micro-morphologies of tensile fracture surfaces and bonding interfaces were studied by SEM (ZEISS Sigma 500) equipped with EDS.

## 2 Experimental

The twin-roll casting experiments were conducted on a  $d160\text{ mm} \times 150\text{ mm}$  twin-roll experimental caster at National Engineering Research Center for Equipment and Technology of Cold Strip Rolling, Yanshan University, China. The schematic diagram for twin-roll casting process of Invar/Cu clad strips is shown Fig. 1. The roller surface needs to be cleaned and sprayed with graphite solution before and during the twin-roll casting experiment. Then, the solid strip of Invar 4J36 and molten copper of Cu T2 were fed into the roll bite of the twin-roll caster simultaneously. The roller surface was cleaned before the twin-roll casting experiment, and the roller surface was sprayed with graphite solution during the twin-roll casting process. Eventually, the Invar/Cu clad strip can be obtained successfully from the roll exit. In the experiment, the tension of the solid strip and contact angle ( $\theta$ ) can be controlled by using a decoiler. Also, the ladle, tundish, and delivery device ensure the continuity and stability of feeding molten copper into the cast-rolling area. After rolling, the diffusion layer with a certain thickness at the bonding interface could improve the adhesive strength of the clad strip. Then, the Invar/Cu clad strips were heat treated at  $800\text{ }^\circ\text{C}$  for 1 h to obtain good interfacial bonding properties.

Chemical compositions of the initial materials and specific experimental parameters are presented in Table 1 and Table 2, respectively. The roll gap is 2.5 mm, and the initial thickness of Invar strip is 0.6 mm. The mass of Cu that was melt and cast is 2.5 kg in every experiment.

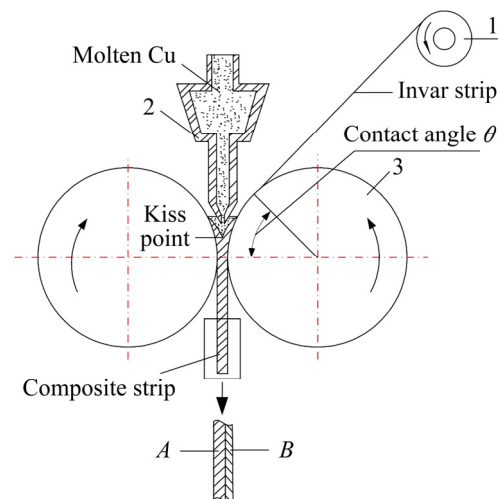


**Fig. 1** Schematic diagram for twin-roll casting process of Invar/Cu clad strip: 1—Decoiler; 2—Delivery device; 3—Twin-roll caster

**Table 1** Chemical composition of materials (mass fraction, %)

Material	Ni	Si	Mn	C	P	S	Fe
Invar	36.7	0.2	0.4	0.05	0.02	0.02	Bal.
Material	Bi	Sb	As	Fe	Pb	S	Cu
Cu	0.001	0.002	0.002	0.005	0.005	0.005	Bal.

**Table 2** Experimental parameters

Parameter	Value
Thickness of Invar/Cu clad strip/mm	2.5
Width of Invar/Cu clad strip/mm	80
Thickness of Invar strip/mm	0.6
Twin-roll casting velocity/( $\text{m} \cdot \text{mm}^{-1}$ )	2.82
Casting temperature of molten Cu/ $^\circ\text{C}$	1200
Casting speed of liquid Cu/( $\text{mm}^3 \cdot \text{min}^{-1}$ )	507000
Initial temperature of Invar strip/ $^\circ\text{C}$	25
Initial temperature of caster roller/ $^\circ\text{C}$	25

Some mechanical tests were followed after the experiments to demonstrate the strip quality. The tensile test and bending test were conducted to evaluate the compatible deformation of Invar/Cu clad strips. Peeling tests were carried out to determine the bonding strength of the clad strips. After the tests, the micro-morphologies of tensile fracture surface and bonding interface were studied by SEM (ZEISS Sigma 500) equipped with EDS. All the test and analysis specimens were sampled from the same clad strip. The sampling locations of each specimen are shown in Fig. 2.

The tensile tests with tensile speed of 2 mm/min were conducted on INSPEKT TABLE 100 universal testing machine according to the GB/T 228–2002. The tensile test specimens were cut into the shape with a total

length of 100 mm and width of 20 mm using a precision wire electrical discharge machine, as shown in Fig. 3.

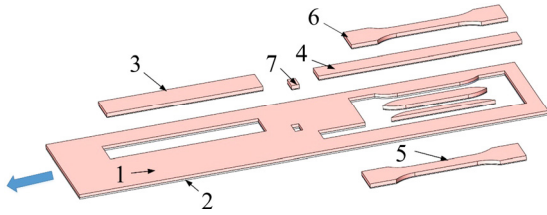


**Fig. 2** Sampling location of specimens (1—Cu; 2—Invar; 3—Specimen for bending test; 4—Specimen for peeling test; 5,6—Specimen for tensile test; 7—Specimen for bonding interface analysis)

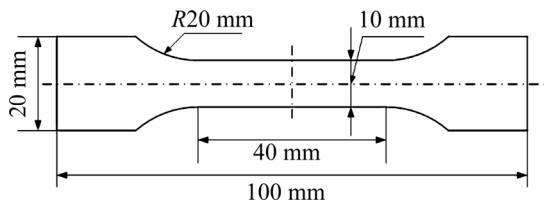


**Fig. 3** Schematic drawing of specimen for tensile test

Bending tests were carried out on DDL 100 universal testing machine according to the GB/T 232–2010 and the specimens were cut into the shape with a total length of 100 mm and width of 20 mm, which are schematically shown in Fig. 4.

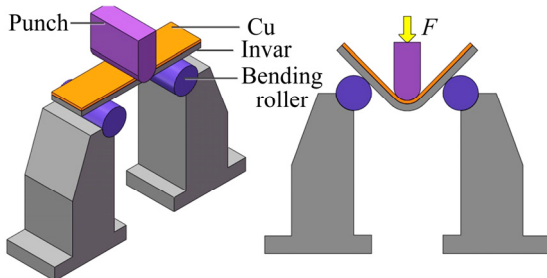


**Fig. 4** Schematic drawing of bending test

T-type peeling tests were conducted according to the ASTM D 1876–08. The tensile speed was 5 mm/min. Peeling test specimens with sizes of 130 mm (rolling direction, RD) × 13 mm (transverse direction, TD) were prepared. Before testing, the samples were first peeled with pliers for a fit thickness for clipping on the tensile machine. The peeling test is schematically shown in Fig. 5. The peeling strength ( $\sigma_p$ ) is given by

$$\sigma_p = P/W \quad (1)$$

where  $P$  is the tensile load and  $W$  is the bonding width.

### 3 Results and discussion

#### 3.1 Microstructures

A clad strip with a length of 1000 mm was

fabricated successfully, as shown in Fig. 6. A good appearance and smooth surface on both sides was obtained. The length of the solidification–deformation zone (setback of the tip) is an essential index for the twin-roll casting procedure. Another experimental method needs to be conducted to measure the length of the solidification–deformation zone [32]. Therefore, the cast-rolling area of the process was obtained in the original state through the emergency stop and quick cooling method. Subsequently, the cast-rolling area was sliced using a precision wire electrical discharge machine. The sliced surface was polished and then corroded with ferric chloride saturated aqueous solution. Since the solidification zone and deformation zone of the cast-rolling area would have different macrostructures, so the macrostructure shown in Fig. 7(a) can be applied to locating the setback of the tip approximately.

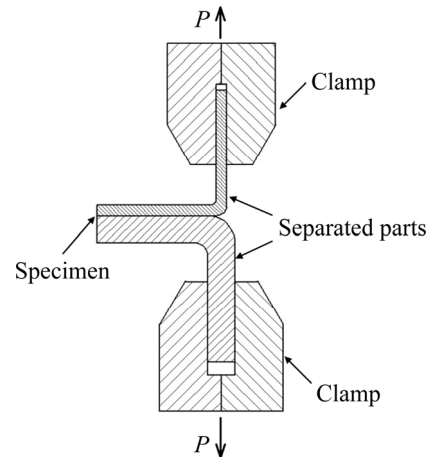


**Fig. 5** Schematic drawing of peeling test

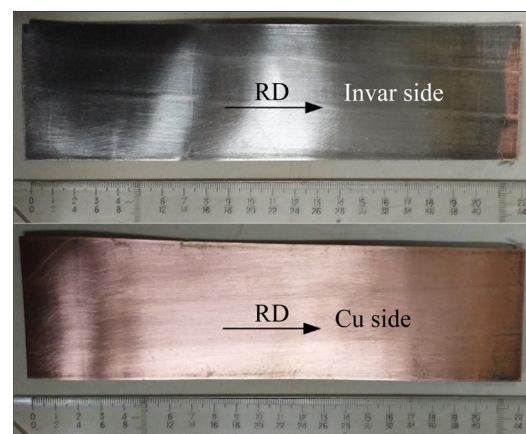


**Fig. 6** Invar/Cu clad strip fabricated by twin-roll casting process

In the solidification zone, the direction of grains would be straight because the growth direction of grains is parallel to and opposite to the direction of heat flow, as shown in Fig. 7(b). Then, the transition between the coarse dendritic and fine equiaxed structures was found

in Fig. 7(c), which indicates the location of the solidification front. After that, the grains would be gradually elongated into slender fibrous structure (Fig. 7(d)) in the deformation zone due to the deformation along rolling direction (RD). Thus, narrow and elongated grains prevail in the finished strip, as shown in Fig. 7(e). The dotted white line in Fig. 7(a) is the boundary between the solidification zone and the deformation zone. The bottom of the dotted line can be considered as the setback of the

tip, and it can also be expressed as the kissing point. Figure 8 shows the microstructures of the as-cast clad strip. Specimens were sampled at the exit of the cast-rolling area and then were mechanically polished and chemically etched. The compositions of the chemical etching solution consist of alcohol, hydrochloric acid and ferric chloride, whose ratio is 20:5:1. It can be seen that the grains of as-cast Cu show long fibrous structure due to the rolling deformation along the rolling direction.

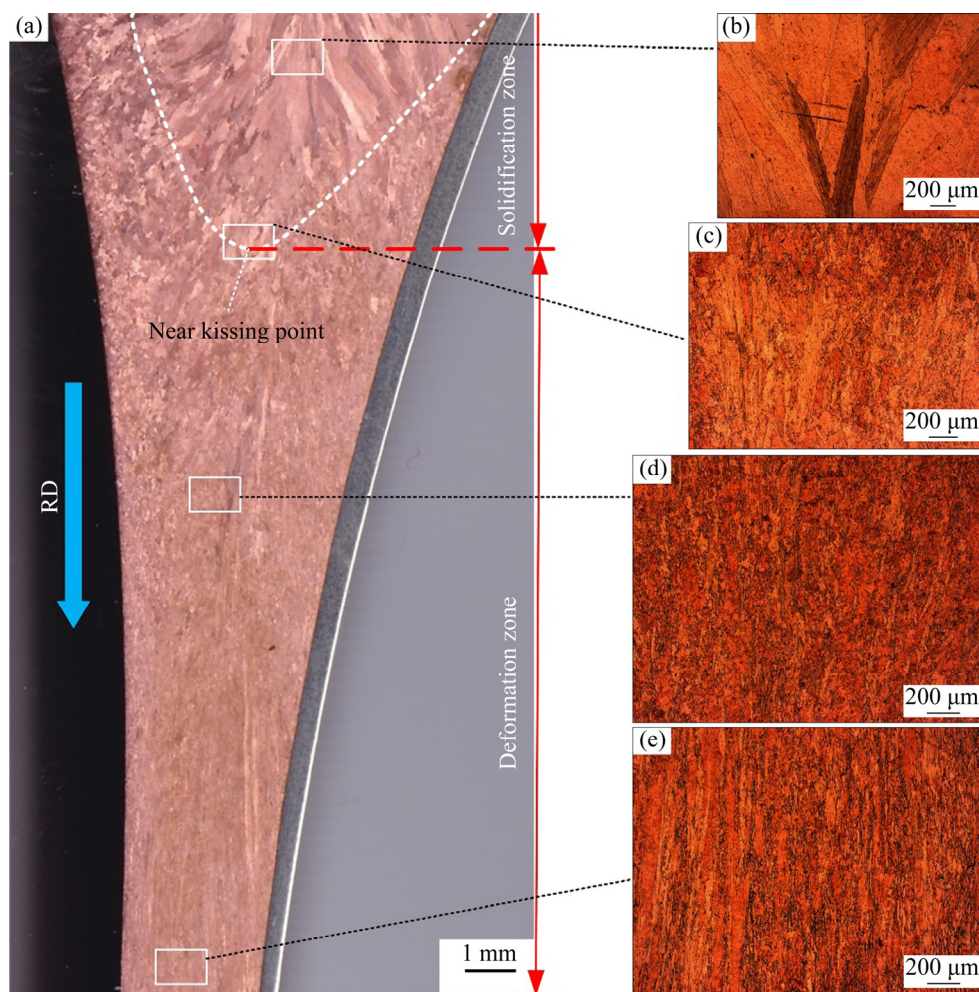


**Fig. 7** Macrostructure of cast-rolling area (a) and microstructures of magnified areas in solidification zone (b), near kissing point (c), in deformation zone (d), and in clad strip (e)

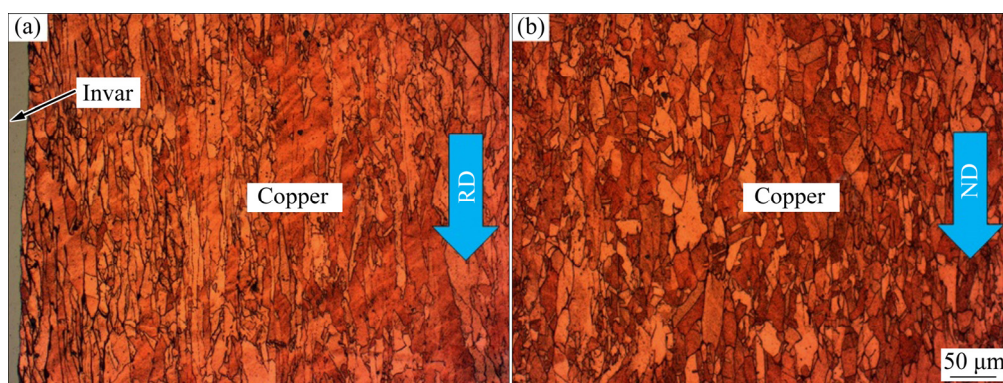


**Fig. 8** Microstructures of Invar/Cu clad strip along RD (a) and ND (b)

Figure 9(a) shows the SEM image of the bonding interface of as-cast Invar/Cu clad strips. It can be seen that the interface is continuous and uniform. No gap or crack is found. EDS line-scan was used to investigate the element diffusion across the interface, and the results are shown in Fig. 9(b). This indicates that the diffusion layer thickness is about 1.6  $\mu\text{m}$ , which means that metallurgical bonding is formed at the interface [33,34]. Only Cu, Fe and Ni were detected at the interface, which demonstrates that the interface has not been oxidized due to the protection of the inert gas during the twin-roll casting process. Besides, from the distribution of Fe and Cu which varies gradually, it could be speculated that there is no obvious intermetallic compound generated at the interface of the as-cast Invar/Cu clad strip [35,36].

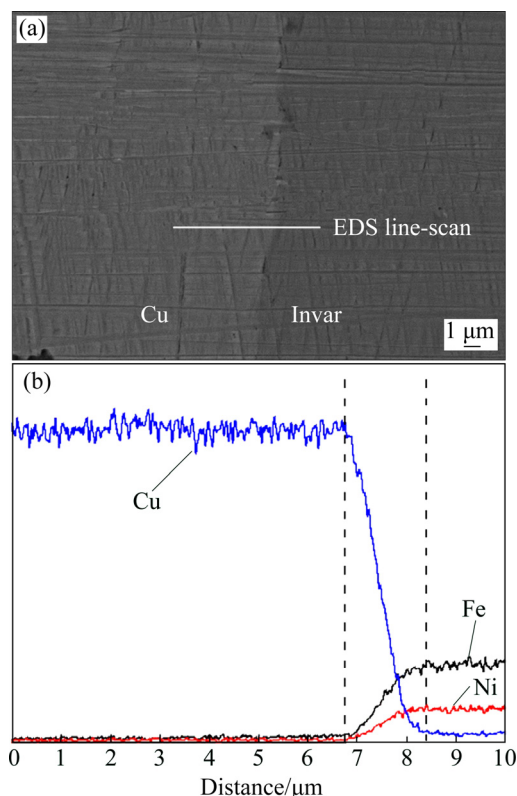


**Fig. 9** Interface of as-cast Invar/Cu clad strips: (a) Microstructure; (b) Element distribution

### 3.2 Uniaxial tensile tests

The tensile engineering stress–strain curves of specimens 1, 2, 3 and 4 which were sampled from the as-cast clad strip are shown in Fig. 10. At the beginning of the test, all load curves are straightened up sharply, and then stabilize gradually during tensile process. However, a sudden decrease of stress is found in the stress–strain curve of specimen 1. Figure 11 shows the macroscopic morphologies of four fractured specimens. It can be seen that the plastic fracture occurs in the range of scale distance and the fractured specimens are necked after obvious plastic deformation. Obvious delamination

phenomenon is found at the specimen 1, but no delamination phenomenon occurs at the specimens 2, 3, 4. Subsequently, the fracture position of the specimen 1 was cut off for further analysis in the precision wire electrical discharge machine. The SEM and EDS mapping images of the Invar alloy are shown in Fig. 12. Only a part of the Invar alloy surface was covered with copper, and the rest part was exposed. This indicated that the bonding interface at the fracture position did not achieve 100% bonding, which is the reason for delamination phenomenon at the bonding interface during uniaxial tensile tests. Plastic fracture occurs at Invar first because Cu has a higher elongation than Invar. Then, Cu is elongated to a certain extent alone, and finally fractured. Therefore, two stress platforms exist in the stress–strain curve of specimen 1. However, Cu and Invar of specimens 2, 3 and 4 are elongated together during the tensile test, and the maximum stress and elongation of specimens 2, 3 and 4 are higher than those of specimen 1.

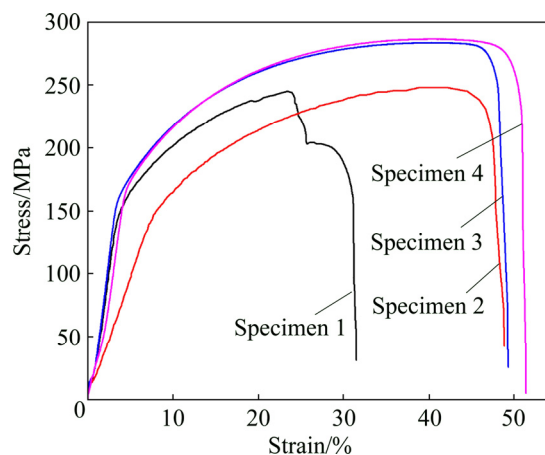


**Fig. 10** Stress–strain curves of Invar/Cu clad strips during tensile test

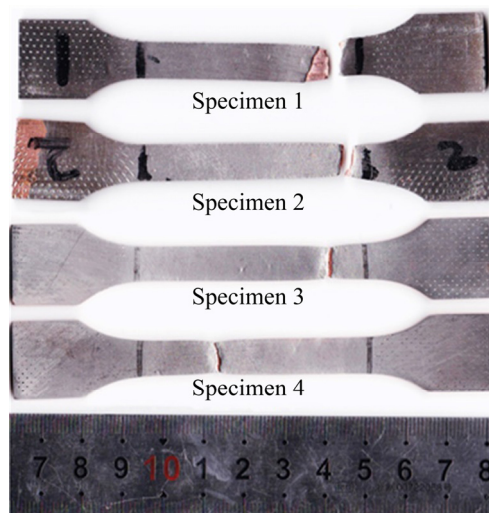


**Fig. 11** Macromorphologies of four tensile test specimens

The fracture microstructures of specimen 2 are shown in Fig. 13. Figure 13(a) shows the SEM image of the fracture. It can be seen that the tensile fracture of the Invar/Cu clad strip is cup-shaped and micro-crack occurs at the bonding interface. The enlarged view of the micro-crack is shown in Fig. 13(b). Slight delamination phenomenon is found near the fracture, and the micro-morphology of the separated interface is the typical ridge-like plastic fracture. The different mechanical properties of Invar and Cu will generate the separation force at the interface during the tensile process. With the constraint of the metallurgical bonding interface, Invar and Cu can deform compatibly at the beginning of the deformation because the separation force is small. With the deformation goes on, separation force is risen to a critical value which exceeds the interfacial bonding strength, so delamination

phenomenon occurs. The tensile fracture micro-morphology of Invar side is shown in Fig. 13(c). Banding and dimple coexist, which indicates that the fracture is plastic fracture. Figure 13(d) shows the tensile fracture micro-morphology of Cu side. There are a large number of evenly distributed equiaxed dimples and part of the ridge-like area. Thus, it can be assumed that the fracture is also plastic fracture.

Therefore, it can be inferred that the main fracture mode of Invar/Cu clad strips prepared by twin-roll casting process is plastic fracture during the uniaxial tensile test. Owing to the constraint of the metallurgical bonding interface, substrate and clad can deform compatibly without the delamination phenomenon during tensile process. Under this circumstance only one stress platform exists in the stress–strain curve. On the contrary, the delamination phenomenon will occur at the

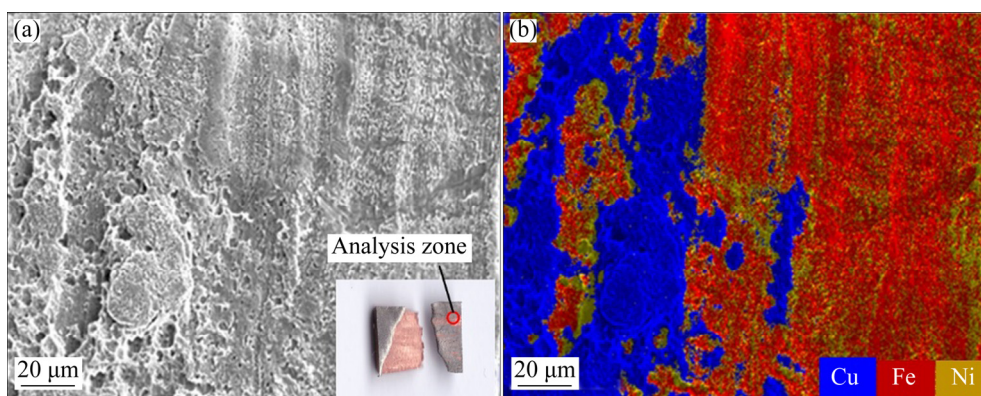


**Fig. 12** Fracture microstructures of specimen 1: (a) SEM image, (b) SEM–EDS mapping image

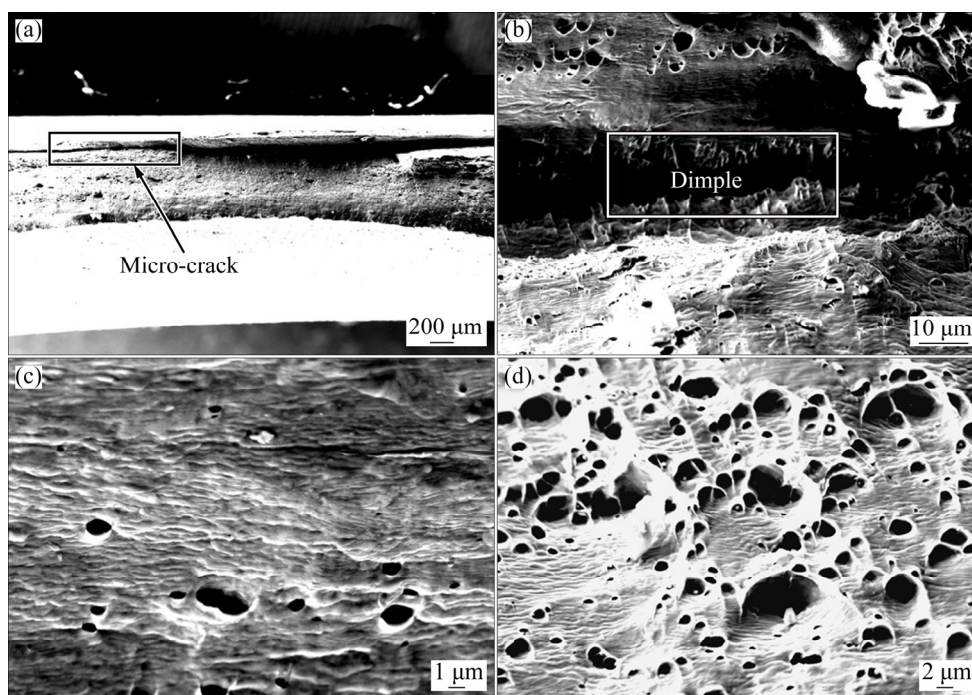


**Fig. 13** Fracture microstructures of specimen 2: (a) Fracture micro-morphology; (b) Enlarged micro-crack; (c) Micro-morphology of Invar side; (d) Micro-morphology of Cu side

positions where 100% bonding is not achieved firstly during the stretching process. Then, substrate and clad will fracture successively, which results in two stress platforms in the stress–strain curve.

### 3.3 Bending test

Figure 14(a) shows the overall appearances of as-cast Invar/Cu clad strips subjected to the excurvation and incurvation bending tests, and the enlarged section morphologies are shown in Fig. 14(b). No delamination or crack occurs at the interface of Invar/Cu clad strips in both excurvation and incurvation bending tests, which demonstrates that the Invar/Cu clad strips fabricated via the twin-roll casting process have desired plastic workability and the substrate and cladding material can deform compatibly.

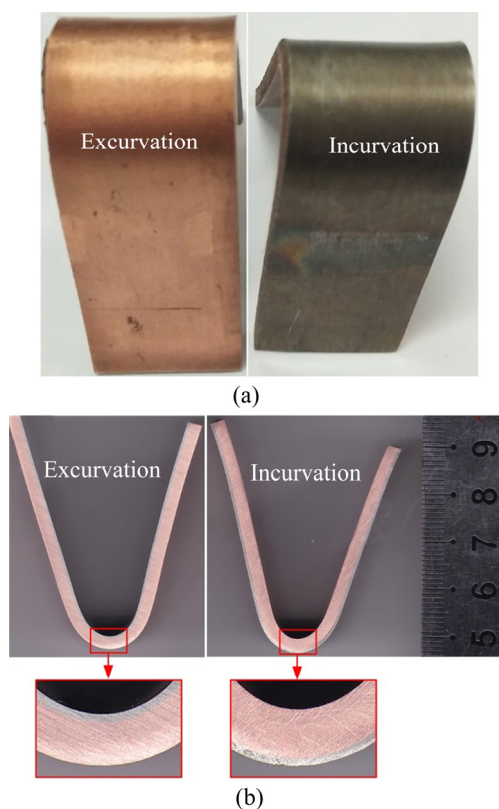


**Fig. 14** Bending test results of as-cast Invar /Cu clad strips: (a) Overall appearances; (b) Section morphologies

### 3.4 Peeling test

Peeling tests for the as-cast Invar/Cu clad strip and the clad strip heat treated at 800 °C for 1h were both conducted, and the obtained peeling strength curves are shown in Fig. 15. This indicates that the curve of as-cast Invar/Cu clad strip has high fluctuation range, and the average peeling force is 180 N. The peeling strength calculated according to Eq. (1) is 13.85 N/mm. On the contrary, the curve of heat treated Invar/Cu clad strip is smooth and steady. The average peeling force is 550 N,

and the peeling strength calculated according to Eq. (1) is 42.31 N/mm. The peeling strength of the heat treated clad strip is significantly improved compared with that of the as-cast one. This indicates that twin-roll casting process provides an efficient way to fabricate Invar/Cu clad strips with desired bonding quality due to the solid–liquid or solid–semisolid reaction and the rolling bonding deformation, and the annealing treatment can be used to improve the bonding strength.

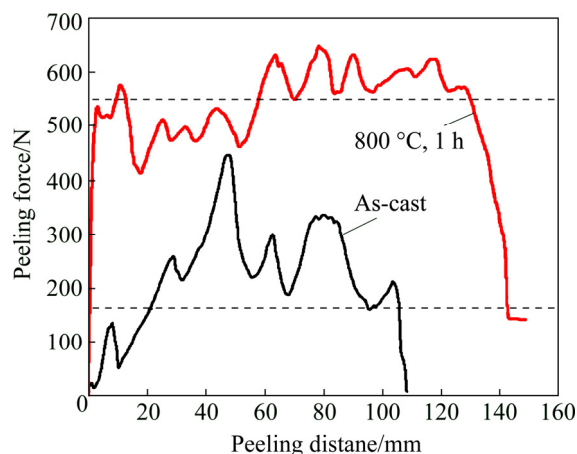


**Fig. 15** Curves of Invar /Cu peeling force

After peeling, the SEM and SEM–EDS mapping images of the as-cast Invar/Cu clad strip interface are shown in Fig. 16. Figures 16(a) and (d) show the micro-morphologies of Invar side and Cu side respectively. A large number of ridge-like dimples exist on both sides, which indicates that it is caused by plastic fracture during the peeling process. However, the ridge-like dimples are not flat, which leads to the large range fluctuation of the peeling force. The EDS surface-scan results on Invar side are shown in Figs. 16(b) and (c). And the EDS surface-scan results on Cu side are shown in Figs. 16(e) and (f). A large amount of Cu element is detected on the top of ridge-like bugles on the Invar side, and a small amount of Fe element is detected on the top of the ridge-like bugles on the Cu side. Therefore, it can be speculated that the plastic fracture takes precedence on the Cu side.

The SEM and SEM–EDS mapping images of the heat treated Invar/Cu clad strip interface are shown in Fig. 17. Figures 17(a) and (d) show the micro-morphologies of Invar side and Cu side after peeling respectively. Peeling surface of Invar side is mainly flat, and there are few ridge-like dimples. The peeling surface of the Cu side is mainly small ridge-like bugles, except for a few large ridge-like dimples. The EDS surface-scan result on the Invar side shows that the lamellar area on the surface contains a large amount of Cu element, as shown in Figs. 17(b) and (c). Figures 17(e) and (f) show that the content of the Fe element on the Cu side is

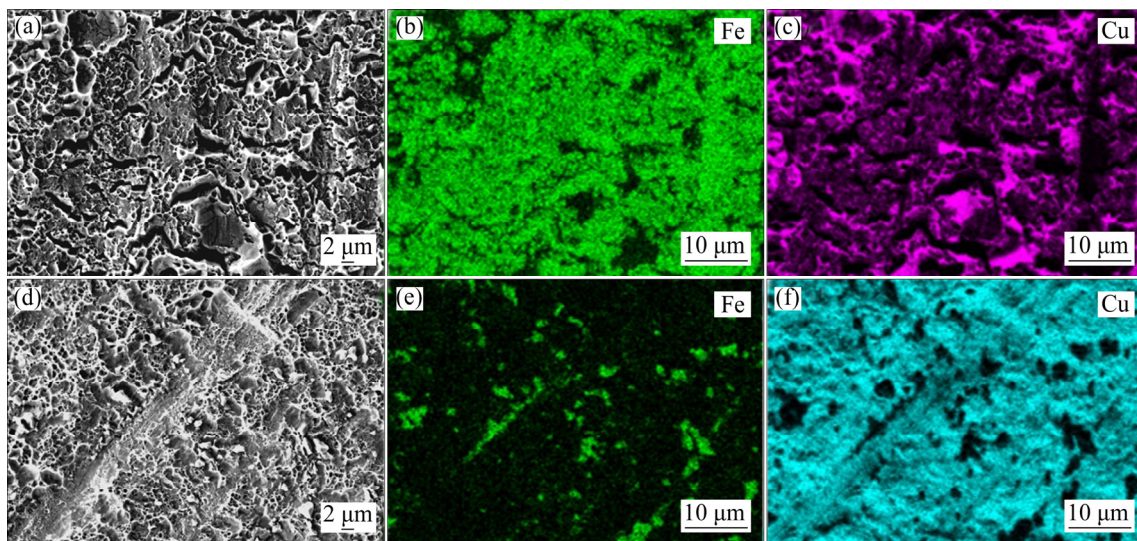


**Fig. 16** SEM (a, d) and SEM-EDS mapping (b, c, e, f) images of as-cast Invar/Cu clad strip interface for Invar side (a, b, c) and Cu side (d, e, f)

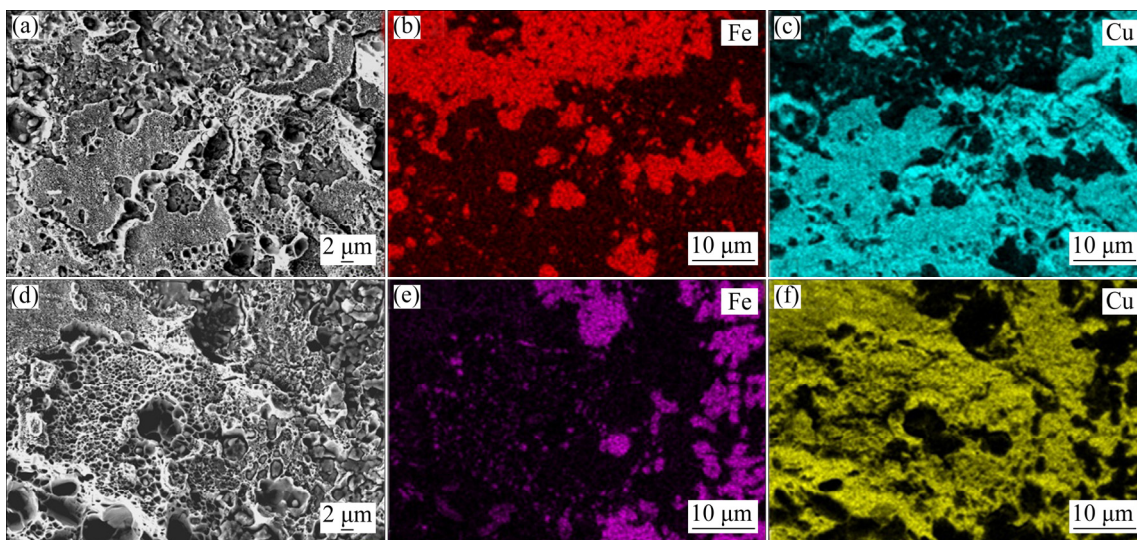


**Fig. 17** SEM (a, d) and SEM-EDS mapping (b, c, e, f) images of annealed Invar/Cu clad strip interface for Invar side (a, b, c) and Cu side (d, e, f)

increased significantly after heat treatment, which means that the bonding interface becomes more homogeneous. Therefore, heat treatment is capable of enhancing the bonding strength and improving the stability of the peeling force.

#### 4 Conclusions

1) For the as-cast Invar/Cu clad strip with sound bonding effect, the tensile strength is about 250 MPa, and only one stress platform exists. However, two stress platforms will be found during the uniaxial tensile tests due to the different mechanical properties of Invar and Cu, when delamination occurs at the bonding interface.

2) No crack or separation occurs at the interface of Invar/Cu clad strips after the excruciation and incurvation

bending tests. Invar/Cu clad strips fabricated via the twin-roll casting process demonstrate desired plastic workability and compatible deformation between substrate and cladding material.

3) The average peeling strength will be increased from 13.85 to 42.31 N/mm after heat treatment at 800 °C for 1 h. Therefore, the bonding adhesive strength of Invar/Cu clad strips will be effectively increased by heat treatment.

#### References

- [1] LI Xiao-Bing, ZU Guo-Yin, WANG Ping. Microstructural development and its effects on mechanical properties of Al/Cu laminated composite [J]. Transactions of Nonferrous Metals Society of China, 2015, 25: 36–45.
- [2] HU Yuan, CHEN Yi-qing, LI Li, HU Huan-dong, ZHU Zi-ang.

- Microstructure and properties of Al/Cu bimetal in liquid–solid compound casting process [J]. *Transactions of Nonferrous Metals Society of China*, 2016, 26: 1555–1563.
- [3] HAGHIGHAT H, SAADATI P. An upper bound analysis of rolling process of non-bonded sandwich sheets [J]. *Transactions of Nonferrous Metals Society of China*, 2015, 25(5): 1605–1613.
- [4] HOSSEINI M, MANESH H D. Bond strength optimization of Ti/Cu/Ti clad composites produced by roll-bonding [J]. *Materials & Design*, 2015, 81: 122–132.
- [5] JING Yu-an, QIN Yi, ZANG Xiao-ming, LI Ying-hong. The bonding properties and interfacial morphologies of clad plate prepared by multiple passes hot rolling in a protective atmosphere [J]. *Journal of Materials Processing Technology*, 2014, 214(8): 1686–1695.
- [6] BYKOV A A. Bimetal production and applications [J]. *Steel in Translation*, 2011, 41(9): 778–786.
- [7] GRYDIN O, SCHAPER M, STOLBCHENKO M. COMPARISON OF Twin-roll casting and high-temperature roll bonding for steel-clad aluminum strip production [C]//*Light Metals*. Orlando, Florida: TMS, 2015: 1225–1230.
- [8] GRYDIN O, GERSTEIN G, NÜRNBERGER F, SCHAPER M, DANCHENKOC V. Twin-roll casting of aluminum–steel clad strips [J]. *Journal of Manufacturing Processes*, 2013, 15(4): 501–507.
- [9] STOLBCHENKO M, GRYDIN O, SAMSONENKO A, KHVIST V, SCHAPER M. Numerical analysis of the twin-roll casting of thin aluminium-steel clad strips [J]. *Forschung im Ingenieurwesen*, 2014, 78: 121–130.
- [10] JAFARIAN M, RIZI M S, JAFARIAN M, HONARMAND M, JAVADINEJAD H R, GHAHERI A, BAHRAMIPOUR M T, EBRAHIMIAN M. Effect of thermal tempering on microstructure and mechanical properties of Mg-AZ31/Al-6061 diffusion bonding [J]. *Materials Science & Engineering A*, 2016, 666: 372–379.
- [11] MA M, HUO P, LIU W C, WANG G J, WANG D M. Microstructure and mechanical properties of Al/Ti/Al laminated composites prepared by roll bonding [J]. *Materials Science & Engineering A*, 2015, 636: 301–310.
- [12] WANG Chun-yang, JIANG Yan-bin, XIE Jian-xin, ZHOU De-jing, ZHANG Xiao-jun. Effect of the steel sheet surface hardening state on interfacial bonding strength of embedded aluminum–steel composite sheet produced by cold roll bonding process [J]. *Materials Science & Engineering A*, 2016, 652: 51–58.
- [13] FRONCZEK D M, WOJEWODA-BUDKA J, CHULIST R, SYPIEN A, KORNEVA A, SZULC Z, SCHELL N, ZIEBA P. Structural properties of Ti/Al clads manufactured by explosive welding and annealing [J]. *Materials & Design*, 2016, 91: 80–89.
- [14] LI Bo, SHEN Yi-fu, LUO Lei, HU Wei-ye. Effects of processing variables and heat treatments on Al/Ti–6Al–4V interface microstructure of bimetal clad-plate fabricated via a novel route employing friction stir lap welding [J]. *Journal of Alloys and Compounds*, 2016, 658: 904–913.
- [15] HAGA T, SUZUKI S. A twin-roll caster to cast clad strip [J]. *Journal of Materials Processing Technology*, 2003, 138(1–3): 366–371.
- [16] HAGA T, KOZONO R, NISHIDA S, WATARI H. Casting of aluminum alloy clad strip by an unequal diameter twin-roll caster equipped with a scraper [J]. *Advances in Materials and Processing Technologies*, 2017, 3(4): 511–521.
- [17] STOLBCHENKO M, GRYDIN O, SCHAPER M. Twin-roll casting of aluminum-steel clad strips: Static and dynamic mechanical properties of the composite [C]//*Light Metals*. San Diego, California: TMS, 2017: 843–851.
- [18] STOLBCHENKO M, GRYDIN O, SCHAPER M. Influence of surface roughness on the bonding quality in twin-roll cast clad strip [J]. *Materials and Manufacturing Processes*, 2018, 33(7): 727–734.
- [19] HUANG Hua-gui, DONG Yi-kang, YAN Meng, DU Feng-shan. Evolution of bonding interface in solid–liquid cast-rolling bonding of Cu/Al clad strip [J]. *Transactions of Nonferrous Metals Society of China*, 2017, 27(5): 1019–1025.
- [20] HUANG Hua-gui, JI Ce, DONG Yi-kang, DU Feng-shan. Thermal-flow coupled numerical simulation and experimental research on bonding mechanism of Cu/Al composite strip by solid-liquid cast-rolling [J]. *The Chinese Journal of Nonferrous Metals*, 2016, 26(3): 623–629.
- [21] BAE J H, RAO A K P, KIM K H, KIM, N. J. Cladding of Mg alloy with Al by twin-roll casting [J]. *Scripta Materialia*, 2011, 64(9): 836–839.
- [22] GRYDIN O, STOLBCHENKO M, SCHAPER M. Impact of steel substrate preheating on microstructure and properties of twin-roll cast aluminium -steel clad strips [C]//*Procedia Engineering*. Cambridge, United Kingdom: ICTP, 2017, 207: 1695–1700.
- [23] STOLBCHENKO M, GRYDIN O, NÜRNBERGER F, SAMSONENKO A, SCHAPER M. Sandwich rolling of twin-roll cast aluminium-steel clad strips [C]//*Procedia Engineering*. Nagoya, Japan: ICTP, 2014: 1541–1546.
- [24] HUANG H G, CHEN P, JI C. Solid-liquid cast-rolling bonding (SLCRB) and annealing of Ti/Al cladding strip [J]. *Materials & Design*, 2017, 118: 233–244.
- [25] VIDONI M, ACKERMANN R, RICHTER S, HIRT G. Production of clad steel strips by twin-roll strip casting [J]. *Advanced Engineering Materials*, 2015, 17(11): 1588–1597.
- [26] MUNSTER D, ZHANG Bo-wen, HIRT G. Processing of clad steel strips consisting of a high manganese and stainless steel pairing produced by twin-roll casting [J]. *Steel Research International*, 2017, 88(1): 1–7.
- [27] COTTLE R D, CHEN X, JAIN R K, ELIEZER Z, RABENBERG L, FINE M E. Designing low-thermal-expansivity, high-conductivity alloys in the Cu–Fe–Ni ternary system [J]. *Journal of the Minerals, Metals and Materials Society*, 1998, 50(6): 67–69.
- [28] STOLK J, MANTHIRAM A. Chemical synthesis and properties of nanocrystalline Cu–Fe–Ni alloys [J]. *Materials Science and Engineering: B*, 1999, 60(2): 112–117.
- [29] WU Dan, YANG Lei, SHI Chang-dong, WU Yu-cheng, TANG Wen-ming. Effects of rolling and on microstructures and properties of Cu/Invar electronic packaging composites prepared by powder metallurgy [J]. *Transactions of Nonferrous Metals Society of China*, 2015, 25(6): 1995–2002.
- [30] WU D, WU S P, YANG L, SHI C D, WU Y C, TANG W M. Preparation of Cu/Invar composites by powder metallurgy [J]. *Powder Metallurgy*, 2015, 58(2): 100–105.
- [31] LIU Ya-jun, ZHANG Li-jun, DU Yong, SHENG Guang, WANG Jiang, LIANG Dong. Atomic mobilities, zero-flux planes and flux reversals in fcc Cu–Fe–Ni alloys [J]. *Calphad*, 2011, 35(3): 376–383.
- [32] GRYDIN O, STOLBCHENKO M, SCHAPER M. Deformation zone length and plastic strain in twin-roll casting of strips of Al–Mg–Si alloy [J]. *The Journal of The Minerals, Metals & Materials Society*, 2017, 69: 1–5.
- [33] CHEN Gang, LI Jin-tao, XU Guang-ming. Bonding process and interfacial reaction in horizontal twin-roll casting of steel/aluminum clad sheet [J]. *Journal of Materials Processing Technology*, 2017, 246: 1–12.
- [34] YU C, XIAO H, YU H, QI Z C, XU C. Mechanical properties and interfacial structure of hot-roll bonding TA2/Q235B plate using DT4 interlayer [J]. *Materials Science & Engineering A*, 2017, 695: 120–125.
- [35] JAFARIAN M, RIZI M S, JAFARIAN M, HONARMAND M, JAVADINEJAD H R, GHAHERI A, BAHRAMIPOUR M T. Effect of thermal tempering on microstructure and mechanical properties of Mg-AZ31/Al-6061 diffusion bonding [J]. *Materials Science & Engineering A*, 2016, 666: 372–379.
- [36] KIM D W, LEE D H, KIM J S, SOHN S S, KIM H S, LEE S. Novel twin-roll-cast Ti/Al clad sheets with excellent tensile properties [J]. *Scientific Reports*, 2017, 7: 1–11.

# 双辊铸轧工艺制备 Invar/Cu 复合带材及其界面结合强度

陈 鹏<sup>1,2</sup>, 黄华贵<sup>1,2</sup>, 季 策<sup>1,2</sup>, 张 旭<sup>1,2</sup>, 孙中华<sup>3</sup>

1. 燕山大学 国家冷轧板带装备及工艺工程技术研究中心, 秦皇岛 066004;
2. 燕山大学 机械工程学院, 秦皇岛 066004;
3. 河钢集团 钢研总院, 石家庄 052165

**摘 要:** 基于传统双辊铸轧工艺将固态因瓦合金(Invar)带材与熔融态铜液同时喂入铸轧机辊缝, 在铸轧区高温、强压和塑性变形共同作用下, 成功制备 Invar/Cu 层状复合带材。通过拉伸、弯曲、T 型剥离及 SEM、EDS 测试, 分析 Invar/Cu 复合带材的力学性能及拉伸断口和结合界面显微形貌。结果表明, 折弯中覆层与基层协调变形, 未出现分层现象; 当界面结合强度较高时, 拉伸应力-应变曲线只有一个应力平台; 相反, 由于 Invar 和 Cu 的力学性能差异, 在等轴拉伸过程中出现界面分层现象, 在两组元发生缩颈时, 应力-应变曲线相应地出现两个应力平台; 经 800 °C 热处理 1 h, 平均剥离强度由铸轧态的 13.85 N/mm 提升至 42.31 N/mm; 并且, 退火处理后 Cu 侧剥离界面 SEM 和 EDS 结果证明, Cu 侧黏连有更多的 Fe, 这说明退火处理可以增强 Invar/Cu 复合带材的界面结合强度。

**关键词:** 双辊铸轧; Invar/Cu 复合带; 热处理; 结合界面; 结合强度

(Edited by Xiang-qun LI)